Journal of Biomolecular NMR, 9 (1997) 136–150
ESCOM

J-Bio NMR 415

Quantitation of chemical exchange rates using pulsed-field-gradient diffusion measurements

Michael Andrec and James H. Prestegard*

Department of Chemistry, Yale University, P.O. Box 208107, New Haven, CT 06520-8107, U.S.A.

Received 26 July 1996
Accepted 21 November 1996

Keywords: Acyl carrier protein; Translational diffusion; Spin echo; Amide exchange; Bound water

Summary

A new approach to the quantitation of chemical exchange rates is presented, and its utility is illustrated with application to the exchange of protein amide protons with bulk water. The approach consists of a selective-inversion exchange HMQC experiment in which a short spin echo diffusion filter has been inserted into the exchange period. In this way, the kinetics of exchange are encoded directly in an apparent diffusion coefficient which is a function of the position of the diffusion filter in the pulse sequence. A detailed theoretical analysis of this experiment indicates that, in addition to the measurement of simple exchange rates, the experiment is capable of measuring the effect of mediated exchange, e.g. the transfer of magnetization from bulk water to an amide site mediated by an internal bound water molecule or a labile protein side-chain proton in fast exchange with bulk water. Experimental results for rapid water/amide exchange in acyl carrier protein are shown to be quantitatively consistent with the exchange rates measured using a selective-inversion exchange experiment.

Introduction

The ability to measure the rate of exchange of NMR-active nuclei between chemically distinct sites is key to the understanding of a wide variety of chemical processes. In addition to direct applications to kinetic mechanisms, the dependence of rates on the energetics and accessibility of pathways can give an insight into the structure and stability of even macromolecular systems. Prominent among the latter applications are those which probe protein structure and stability through the rates of exchange of amide protons with protons of water (Englander and Kallenbach, 1984). In these applications, the water protons are normally assumed to belong to a single bulk pool. But, it is clear that in many cases exchange will not be directly with bulk water, but will be mediated by protons from discrete water molecules immobilized in protein cavities or exchangeable protons on side-chain functional groups (Gerothanassis, 1994; Billeter, 1995; Bryant, 1996). The characterization of participation by such intermediate species can provide details of structure and stability well beyond those available from the simple measurement of bulk water exchange. An improved procedure for the measurement of the rates of exchange by both direct and indirect processes is presented here.

When the exchange of protons such as amide protons is slow, the rates can conveniently be monitored by the sequential acquisition of spectra after dilution in deuterated solvent. However, when the exchange is rapid, other methods are needed. It has been possible to make measurements of more rapid rates using experiments which detect magnetization transfer after selective labeling of the magnetization of one of the exchanging species (Gemmecker et al., 1993; Grzesiek and Bax, 1993; Andrec et al., 1995). Such an experiment may involve the inversion of a resonance associated with one of the species, e.g. the bulk water resonance. We call this selective-inversion exchange spectroscopy. A prerequisite for application of this experiment is chemical shift resolution of the resonances belonging to the exchanging sites. Amide proton resonances of a protein are clearly resolved from the bulk water resonance, making this experiment applicable, but the intermediate sites mentioned above often are not. They may have chemical shifts very close to that of bulk

*To whom correspondence should be addressed.

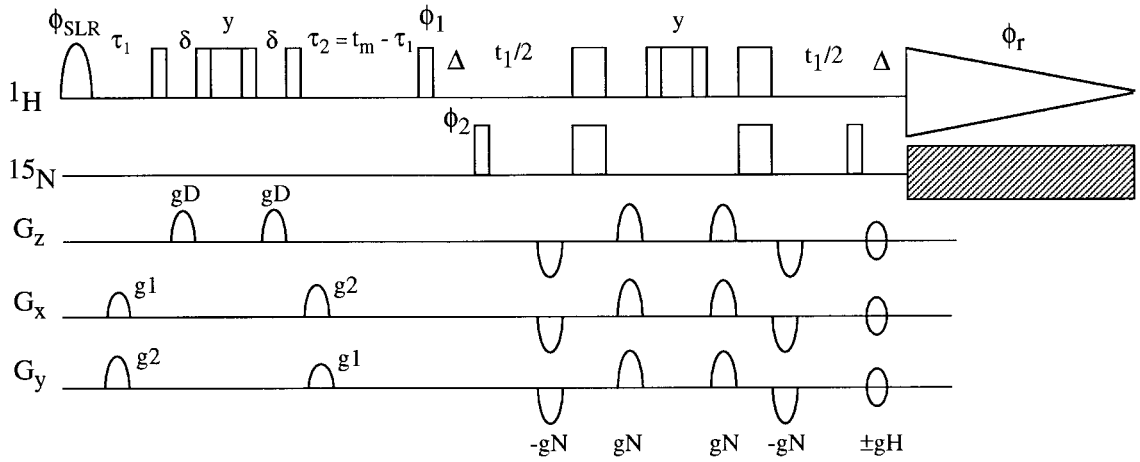

Fig. 1. Pulse sequence for the diffusion-exchange experiment discussed. Narrow and wide rectangles indicate 90° and 180° pulses, respectively, and all rf phases are x unless otherwise indicated. The initial selective ^{1}H pulse is a Shinnar–Le Roux inversion pulse (Shinnar et al., 1989; Pauly et al., 1991) of 50 ms duration. The total mixing time t_m was kept constant at 60 ms. Diffusion gradients gD were a nominal 2.9 or 29.0 G/cm, each lasting 4 ms with 50 μs sinusoidal rise and fall time to reduce eddy current effects. Spoil gradients g1 and g2 were 3 and 6 G/cm, respectively. Coherence-selection gradients gN and gH had a net resultant gradient of 46.7 and 18.9 G/cm, respectively. Bipolar coherence-selection encode gradients were used to improve water suppression, and the coherence-selection decode gradient gH was alternated in sign to allow the restoration of pure-phase line shapes (Tolman et al., 1992). Nitrogen decoupling during acquisition was achieved using GARP modulation (Shaka et al., 1985). Phase cycling: $\phi_1 = 32(x,x,-x,-x)$, $\phi_2 = 32(x,-x,x,-x)$, $\phi_r = 16(x,-x,-x,x),16(-x,x,x,-x)$, $\phi_{SLR} = 4(x),4(y),4(-x),4(-y)$.

water or they may be in rapid exchange with bulk water so that their resonances are averaged with the bulk water resonance. This makes direct detection of intermediate steps in the exchange process difficult by simple application of magnetization transfer experiments. To surpass this difficulty, one must use a physical property other than chemical shift to resolve the exchanging species. Since many exchange and ligand binding processes of interest in biophysics involve modulation of the translational diffusion coefficient by an order of magnitude or more, molecular diffusion could, in principle, be used to resolve steps in the exchange or binding processes. Experiments to that end have been proposed (Moonen et al., 1992; Kriwacki et al., 1993; Dötsch and Wider, 1995).

The measurement of translational diffusion using spin echoes and magnetic field gradients has been known for several decades (Hahn, 1950; Stejskal and Tanner, 1965). However, only recently has it become clear that diffusion can be used as a resolution aid. A prime example is the 'diffusion-ordered spectroscopy' (DOSY) approach of Johnson and co-workers (Morris and Johnson, 1992,1993), which has been fruitfully applied to such problems as the determination of vesicle size distributions (Hinton and Johnson, 1993) and binding isotherms (Chen et al., 1995). With actively shielded gradient probes now available commercially, there has been a marked increase in interest in the measurement of translational diffusion coupled with high-resolution spectroscopy, including the study of dimerization and aggregation equilibria of biological macromolecules (Altieri et al., 1995; Dingley et al., 1995; Lin and Larive, 1995).

In this paper, we propose a new experiment which combines the advantages of spin echo diffusion measurement and selective-inversion exchange spectroscopy. This diffusion/exchange experiment is a variant of the selective-inversion exchange HMQC difference experiment proposed by Kriwacki et al. (1993). In that experiment a spin echo diffusion element was inserted between the water inversion pulse and the exchange period t_m. This diffusion filter consisted of gradient pulses which dephased transverse magnetization in a spatially dependent fashion, separated by a 180° refocussing pulse. If molecules remain in the same position in space during the spin echo period (i.e. the diffusion constant is small), their magnetization is completely refocussed. If the molecules move (i.e. the diffusion constant is large), then magnetization will not be completely refocussed. Hence this spin echo element acts to filter magnetization based on diffusion constant. Amide proton resonances whose magnetization originated on water and were refocussed in the diffusion filter were selectively detected by a (^{1}H-^{15}N) HMQC element.

In the experiment presented here, a short spin echo diffusion element of length 2δ has been inserted into a mixing period of fixed duration at a variable position defined by the parameter τ_1 (Fig. 1). The total length of the mixing period t_m is kept constant and the ratio of signals in the presence and absence of the gradient gD, $A(\tau_1)/A_0(\tau_1)$, is measured as a function of τ_1. We show that this experiment can be used to characterize the exchange process in terms of the mobility of the species involved if the exchange process is in the limit of slow exchange on the chemical shift timescale. Furthermore, we demonstrate that this method could be used to quantitate chemical exchange which is fast on the chemical

$$A \underset{k_r}{\overset{k_f}{\rightleftharpoons}} B$$

Scheme 1. Two-state exchange.

shift timescale, provided that this exchange is followed by a second exchange process which is slow on the chemical shift timescale. These are conditions that are likely to be fulfilled when bound water or exchangeable side-chain protons mediate amide proton exchange with bulk water.

Theory

Two-state exchange

To lay the groundwork for our discussion, let us first consider the simple case of two-site exchange, where the exchange is slow on the chemical shift timescale and the resonances of the two sites are resolved in chemical shift (see Scheme 1). Here we selectively invert B and observe A. To simplify the analysis, we will consider only the limit $\delta \ll 1/k_f$, $\delta \ll 1/k_r$, so that exchange during the spin echo period can be neglected. We also use the approximation that the diffusion gradients fill the entire spin echo period. In this limit, it can be shown that the magnetization of species i is attenuated by a factor Ψ_i (Hahn, 1950):

$$\Psi_i = \exp\left(-\frac{2}{3}\gamma^2 g^2 D_i \delta^3\right)$$

To evaluate the diffusion attenuation, $A(\tau_1)/A_0(\tau_1)$, we calculate the magnetization of species A at the end of the mixing period in each of four cases: no selective inversion pulse and no diffusion gradients ($M_A^{(0)}$); no selective inversion pulse with diffusion gradients ($M_A^{(g)}$); selective inversion pulse but no diffusion gradients ($M_A^{(i)}$); and both selective inversion pulse and diffusion gradients ($M_A^{(ig)}$). The observed attenuation is defined as

$$\frac{A(\tau_1)}{A_0(\tau_1)} = \frac{M_A^{(g)}(t_m) - M_A^{(ig)}(t_m)}{M_A^{(0)}(t_m) - M_A^{(i)}(t_m)} \qquad (1)$$

In calculating the $M_A(t_m)$ values, we will assume that the equilibrium magnetizations of A and B are equal to their fractional populations p_A and p_B:

$$p_A = \frac{k_r}{k_r + k_f}$$

$$p_B = \frac{k_f}{k_r + k_f}$$

Given initial magnetizations $M_A(0)$ and $M_B(0)$, the magnetization at time t is given by

$$\begin{pmatrix} M_A(t) \\ M_B(t) \end{pmatrix} = \exp(-\mathbf{K}t)\begin{pmatrix} M_A(0) \\ M_B(0) \end{pmatrix} \qquad (2)$$

where the exchange matrix **K** in the limit of the spin-lattice relaxation times of A and B being much longer than t_m is given by

$$K = \begin{pmatrix} k_f & -k_r \\ -k_f & k_r \end{pmatrix}$$

The matrix exponential can easily be evaluated in closed form to give

$$\begin{pmatrix} M_A(t) \\ M_B(t) \end{pmatrix} = \begin{pmatrix} p_B e^{-\lambda t} + p_A & p_A(1 - e^{-\lambda t}) \\ p_B(1 - e^{-\lambda t}) & p_A e^{-\lambda t} + p_B \end{pmatrix}\begin{pmatrix} M_A(0) \\ M_B(0) \end{pmatrix} \qquad (3)$$

where $\lambda = k_r + k_f$. In the absence of gradients, the magnetizations $M_A^{(0)}$ and $M_A^{(i)}$ follow directly from Eq. 3 using initial conditions (p_A, p_B) and $(p_A, -p_B)$ for $M_A^{(0)}$ and $M_A^{(i)}$, respectively:

$$M_A^{(0)}(t_m) = p_A$$

$$M_A^{(i)}(t_m) = p_A\left[p_A + p_B(2e^{-\lambda t_m} - 1)\right]$$

In the presence of the diffusion gradients, we must apply Eq. 3 successively to the time intervals before and after the spin echo. The magnetization at the end of τ_1 is given by Eq. 3 using initial boundary conditions as described above. If we assume that the spin echo is short, the initial boundary conditions for the time period $t_m - \tau_1$ is simply the magnetization at the end of τ_1 attenuated by Ψ_A or Ψ_B for M_A and M_B, respectively. The net result at t_m is

$$M_A^{(g)}(t_m) = p_A\left[p_B e^{-\lambda(t_m - \tau_1)}(\Psi_A - \Psi_B) + p_A\Psi_A + p_B\Psi_B\right]$$

$$M_A^{(ig)}(t_m) = p_A\Psi_A\left(p_A + p_B e^{-\lambda(t_m - \tau_1)}\right)\left[p_A + p_B(2e^{-\lambda\tau_1} - 1)\right] + p_A p_B \Psi_B\left(1 - e^{-\lambda(t_m - \tau_1)}\right)\left[p_B + p_A(2e^{-\lambda\tau_1} - 1)\right]$$

Substitution of all four magnetization terms into Eq. 1 yields

$$\frac{A(\tau_1)}{A_0(\tau_1)} = \frac{(\Psi_A - \Psi_B)\left(p_B e^{\lambda\tau_1} - p_A e^{\lambda(t_m - \tau_1)}\right)}{e^{\lambda t_m} - 1} + \frac{(p_A\Psi_A + p_B\Psi_B)e^{\lambda t_m} - (p_B\Psi_A + p_A\Psi_B)}{e^{\lambda t_m} - 1} \qquad (4)$$

For the applications discussed here, B is a large pool of bulk water, and $p_A \to 0$. In this limit Eq. 4 reduces to a simple exponential function of τ_1. As p_A increases, the function acquires a characteristic sigmoidal shape, as depicted in Fig. 2. For small values of τ_1, where the diffusion filter is applied before any exchange mixing can

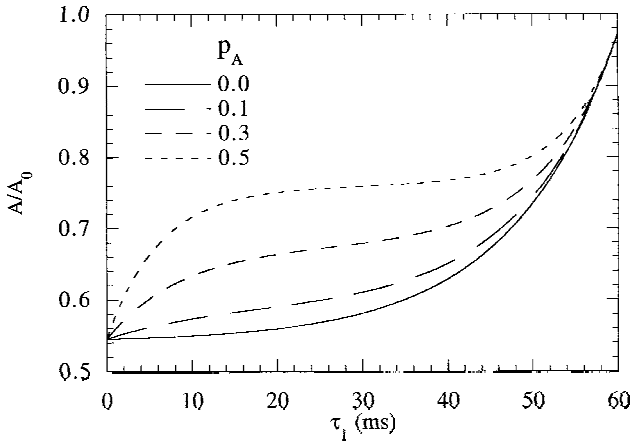

Fig. 2. Theoretically predicted diffusion attenuation profiles as a function of τ_1 for a general two-state exchange process (Scheme 1), neglecting exchange during the spin echo, calculated using Eq. 4 for various fractional populations of the observed species A. A/A_0 is the ratio of signal intensities at gD = 30 G/cm and gD = 0 G/cm. The following parameters were used: $t_m = 60$ ms, $D_A = 0.1$ μm²/ms, $D_B = 2.2$ μm²/ms, $[B]/[A] = 10^4$, $k_f = 80$ s^{-1}, and $\delta = 4$ ms.

occur, the attenuation depends only on Ψ_B (the attenuation of the inverted species). For large values of τ_1 (i.e. $\tau_1 \rightarrow t_m$), where the diffusion filter is applied after the maximum extent of exchange mixing has occurred, the attenuation depends only on Ψ_A (the attenuation of the observed species). For intermediate values of τ_1, the observed attenuation is a mixture of Ψ_A and Ψ_B, which depends on the rate of exchange. In the $p_A \rightarrow 0$ limit, the exchange rate dependence is straightforward. If the exchange rate is fast, Ψ_B will dominate through most of the range of τ_1 values and then there will be an abrupt increase in Ψ_A. Thus, for the accurate quantitation of fast rates (an order of magnitude faster than t_m^{-1}), it would be wise to spend more of the available experimental time collecting data at longer τ_1 values where most of the exchange rate information resides. If the rate is slow (an order of magnitude slower than t_m^{-1}), then exchange occurs irreversibly and uniformly throughout the mixing period, resulting in a nearly linear mixture of Ψ_A and Ψ_B as a function of τ_1 (Fig. 3a). This also limits the ability to differentiate between different slow rates, resulting in less exchange rate resolution as the exchange rate approaches zero. However, between these limits it is clear that the curvature of a plot of A/A_0 versus τ_1 will allow the estimation of an exchange rate.

If exchange events during the spin echo must be considered, then calculation of the diffusion attenuation becomes nontrivial. When one of the species is in vast excess, as is normally the case in amide exchange, the effect of exchange during the spin echo may be determined in closed form. If the concentrations of A and B are not vastly different, we may determine an effective diffusion attenuation for each species by generating random exchange events during the spin echo in a Monte Carlo fashion, and calculating the average of the spin echo diffusion attenuation over all exchange events. The details of such calculations are given in the Appendix, and the effect on the predicted diffusion attenuation is shown in Fig. 3b. The diffusion attenuation deviates from Ψ_B for short τ_1 at slow exchange rates and from Ψ_A for $\tau_1 \approx t_m$ at fast exchange rates. Although the qualitative behavior of the diffusion attenuation as a function of τ_1 is unchanged, the effect of exchange during the spin echo must be considered if an accurate quantitation of exchange rates is desired.

Three-state exchange

It is clear from Eq. 4 and the profiles in Figs. 2 and 3 that one could determine an exchange rate constant k for any two-site process where the species involved have different diffusion constants and exchange is slow enough that spins on one of the sites can be selectively excited.

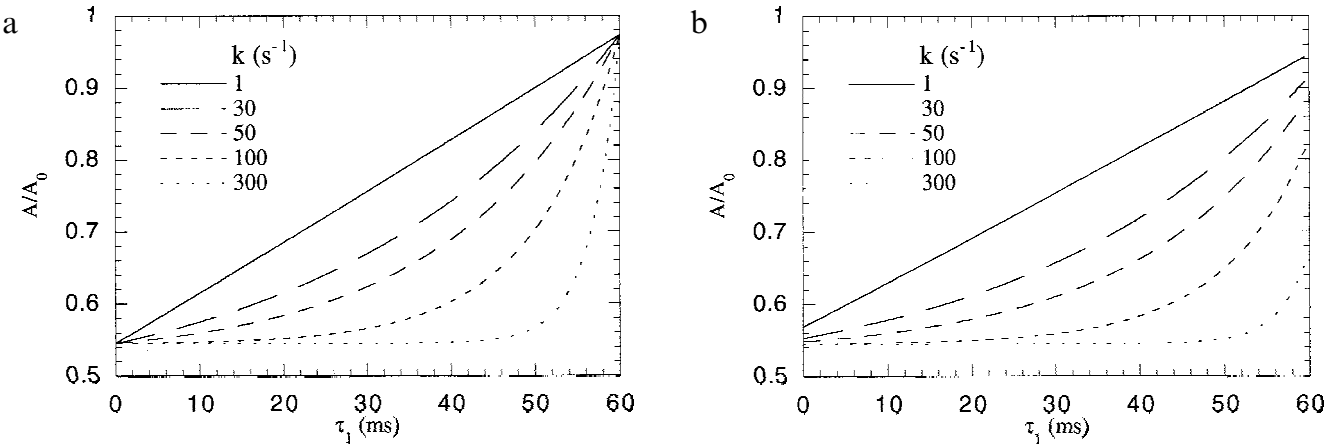

Fig. 3. Theoretically predicted diffusion attenuation profiles as a function of τ_1 and exchange rate k for a two-state exchange process (Scheme 1) where the inverted species is in vast excess. Parameters are the same as in Fig. 2. (a) Theoretical diffusion attenuations, neglecting exchange during the spin echo, calculated using the $p_A \rightarrow 0$ limit of Eq. 4. (b) Theoretical diffusion attenuations calculated using Eq. A8. The definite integrals were evaluated numerically using Romberg quadrature (Press et al., 1992).

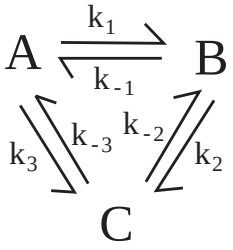

Scheme 2. General three-state exchange.

However, it is often of greater interest to observe the exchange of a third site (such as immobilized water or protons on functional groups) which exchanges rapidly with water. This suggests that considering a system undergoing three-site exchange, in which two of the sites are not easily distinguishable by chemical shift, would be a useful exercise. Such a system is depicted in Scheme 2. In all of the cases considered in this paper, species B and C are selectively inverted and species A is observed.

For the general three-state exchange process shown in Scheme 2, the exchange matrix **K** will be

$$\mathbf{K} = \begin{pmatrix} k_1+k_3 & -k_{-1} & -k_{-3} \\ -k_1 & k_{-1}+k_2 & -k_{-2} \\ -k_3 & -k_2 & k_{-2}+k_{-3} \end{pmatrix}$$

To ensure numerical stability, we apply the similarity transformation $\mathbf{K}_s = \mathbf{S}^{-1}\mathbf{K}\mathbf{S}$ (Moseley et al., 1995),

$$\mathbf{S} = \begin{pmatrix} \sqrt{[A]} & 0 & 0 \\ 0 & \sqrt{[B]} & 0 \\ 0 & 0 & \sqrt{[C]} \end{pmatrix}$$

The result

$$\mathbf{K}_s = \begin{pmatrix} k_1+k_3 & -k_{-1}\sqrt{[B]/[A]} & -k_{-3}\sqrt{[C]/[A]} \\ -k_1\sqrt{[A]/[B]} & k_{-1}+k_2 & -k_{-2}\sqrt{[C]/[B]} \\ -k_3\sqrt{[A]/[C]} & -k_2\sqrt{[B]/[C]} & k_{-2}+k_{-3} \end{pmatrix}$$

is symmetric by virtue of the relations $k_1[A] = k_{-1}[B]$, $k_2[B] = k_{-2}[C]$, and $k_3[A] = k_{-3}[C]$ which follow from microscopic reversibility at the point of chemical equilibrium. The eigenvectors of $\mathbf{K}_s$ are orthonormal, and the time evolution is given by

$$\mathbf{M}(t) = \mathbf{S}\mathbf{T}\exp(-\Lambda t)\,\mathbf{T}^{\dagger}\mathbf{S}^{-1}\mathbf{M}(0) \qquad (5)$$

where $\mathbf{T}\Lambda\mathbf{T}^{\dagger}$ is the eigendecomposition of $\mathbf{K}_s$. Although the eigendecomposition of a 3×3 matrix can, in principle, be done in closed form, it is much more convenient to do the calculation numerically.

For purposes of illustration, we will show the results of such a calculation for one case of particular interest, where species B and C are in fast exchange so they cannot normally be resolved in an NMR spectrum, and A and B are in slow exchange on the chemical shift timescale. A and C are assumed not to directly exchange (Scheme 3). In addition, we will assume that A and B have the same diffusion constant (i.e. they are bound to the same macromolecular species), that the concentration of C is much larger than that of A and B, and that species A is observed after selective inversion of B and C (i.e. species B is an unobservable bound species that mediates magnetization transfer).

The rate constant k_2 corresponds to the fast-exchange process, while k_1 is the rate of the slow-exchange step. In principle, this could be either another chemical exchange or cross-relaxation between spins. The expected diffusion attenuation profiles as a function of τ_1 in the narrow spin echo limit, calculated using Eqs. 1 and 5, are shown in Fig. 4a. For the range depicted, the shapes of the curves depend on both k_1 and k_2 in a way that, in principle, would allow their separation if k_1 or the overall transfer rate can be determined independently. Although k_1 may be difficult to measure directly in all cases, the overall transfer rate from C to A can easily be measured using a selective-inversion exchange experiment such as that used previously by Andrec et al. (1995). If k_1 is rate-limiting, as it is likely to be for the case of cross-relaxation from an immobilized water molecule, it will dominate the overall transfer rate and can be easily measured.

The effect of exchange during the spin echo can be assessed for the case shown in Scheme 3. The contribution from the A⇌B magnetization transfer process is eliminated by the 180° pulse in the middle of the spin echo as long as δ is fairly short. Clearly, the spin echo attenuation of A will then be governed only by D_{ab}, while that of C will be dominated by D_c due to the vast excess of species C. The effective attenuation of B will deviate from that of A to a degree dependent on the exchange rate k_2 and the length of the spin echo 2δ. In the concentration limits assumed here, the effective attenuation can be determined in closed form and is derived in the Appendix. The evalu-

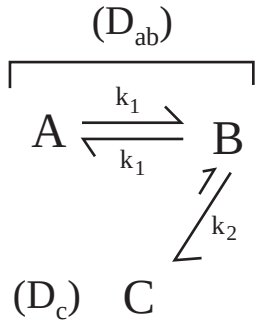

Scheme 3. Mediated three-state exchange.

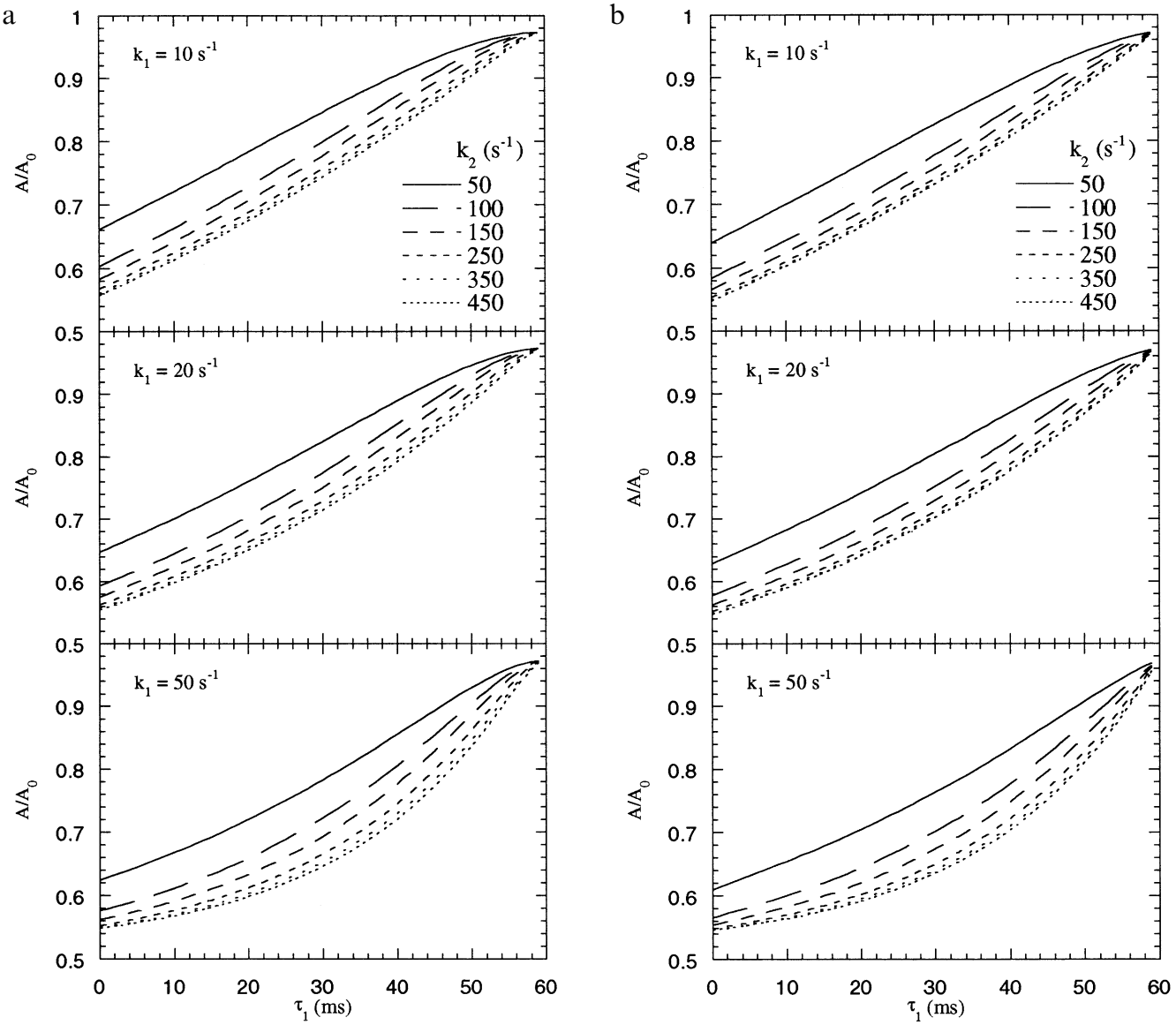

Fig. 4. Theoretically predicted diffusion attenuation profiles as a function of τ_1 and exchange rates k_1 and k_2 for the three-state exchange process shown in Scheme 3. The following parameters were used: $t_m = 60$ ms, $D_{ab} = 0.1$ μm^2/ms, $D_c = 2.2$ μm^2/ms, [C]/[B] = [C]/[A] = 10^4, $\delta = 4$ ms, and gD = 30 G/cm. (a) Theoretical diffusion attenuations, neglecting exchange during the spin echo, calculated using Eqs. 1 and 5. (b) Theoretical diffusion attenuations calculated using Eqs. 1, 5, and A9 as described in the text. The diagonalization of the symmetrized exchange matrix was performed using the Jacobi rotation algorithm (Press et al., 1992).

ation of that result (Eq. A9) for the exchange rates of Fig. 4 shows that Ψ_B varies from 0.6 to 0.9. Despite that, the attenuation profiles as a function of τ_1 are qualitatively identical, as can be seen in Fig. 4b. Thus, with the use of the proper simulation procedure, it is not necessary to make the length of the spin echo short compared to the mean exchange lifetimes. This is a distinct advantage, as many spectroscopists do not have access to specialized hardware which would allow them to operate in the 'narrow-gradient' limit and still achieve measurable diffusion attenuations.

Another case of interest is the situation in which magnetization transfer occurs through a superposition of intermolecular exchange and intramolecular cross-relaxation. A common example of this is the buildup of magnetization on an amide proton in a selective-inversion exchange experiment which arises from simultaneous exchange with bulk water and cross-relaxation with an α-proton which is degenerate in chemical shift with water. This is simply another special case of the general three-state exchange process (Scheme 4), and the attenuation profiles can be calculated using the formalism described above. The qualitative behavior of the attenuation profiles for this case can be easily understood without the need for detailed calculations. In general, signals which arise from a superposition of exchange and cross-relax-

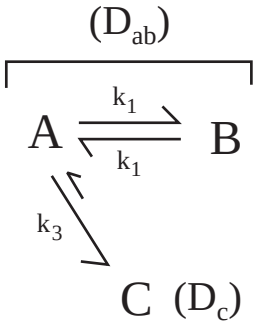

Scheme 4. Three-state exchange with superimposed pathways.

ation are less attenuated than would be expected for direct exchange with bulk water. If the signals arise solely from cross-relaxation, the attenuation profiles will show a τ_1-independent attenuation corresponding to that of protein diffusion. Thus, the diffusion attenuation at short τ_1 values is related to the relative contributions of exchange and cross-relaxation to the observed signal. In principle, this would allow for the unambiguous quantitation of both the NOE and exchange rates.

Materials and Methods

Acyl carrier protein (ACP) was chosen as a suitable macromolecule to test the proposed experiment. The protein was overexpressed in minimal medium using 1 g/l of $^{15}NH_4Cl$ as the sole nitrogen source. Cells were harvested and the ACP was purified using previously published methods, including the HPLC separation of the *holo* and *apo* forms (Andrec et al., 1995; Hill et al., 1995). Only the *apo* form was used in this study. The NMR sample (≈3 mM in ACP) was prepared in an H_2O buffer containing 25 mM 1,3-bis[tris(hydroxymethyl)methylamino]propane, 10 mM $CaCl_2$, and 0.2 mM dithiothreitol (pH 7.2). The sample height was 1.0 cm in a susceptibility-matched NMR tube (Shigemi Co. Ltd., Tokyo, Japan).

All NMR spectra were obtained at 500 MHz proton frequency using a General Electric Omega spectrometer equipped with an S-17 pulsed-field-gradient accessory. Diffusion experiments were performed using a General Electric water-cooled three-axis gradient probe, having a maximum gradient strength along the z-axis of 29 G/cm as estimated by measurement of the diffusion attenuation

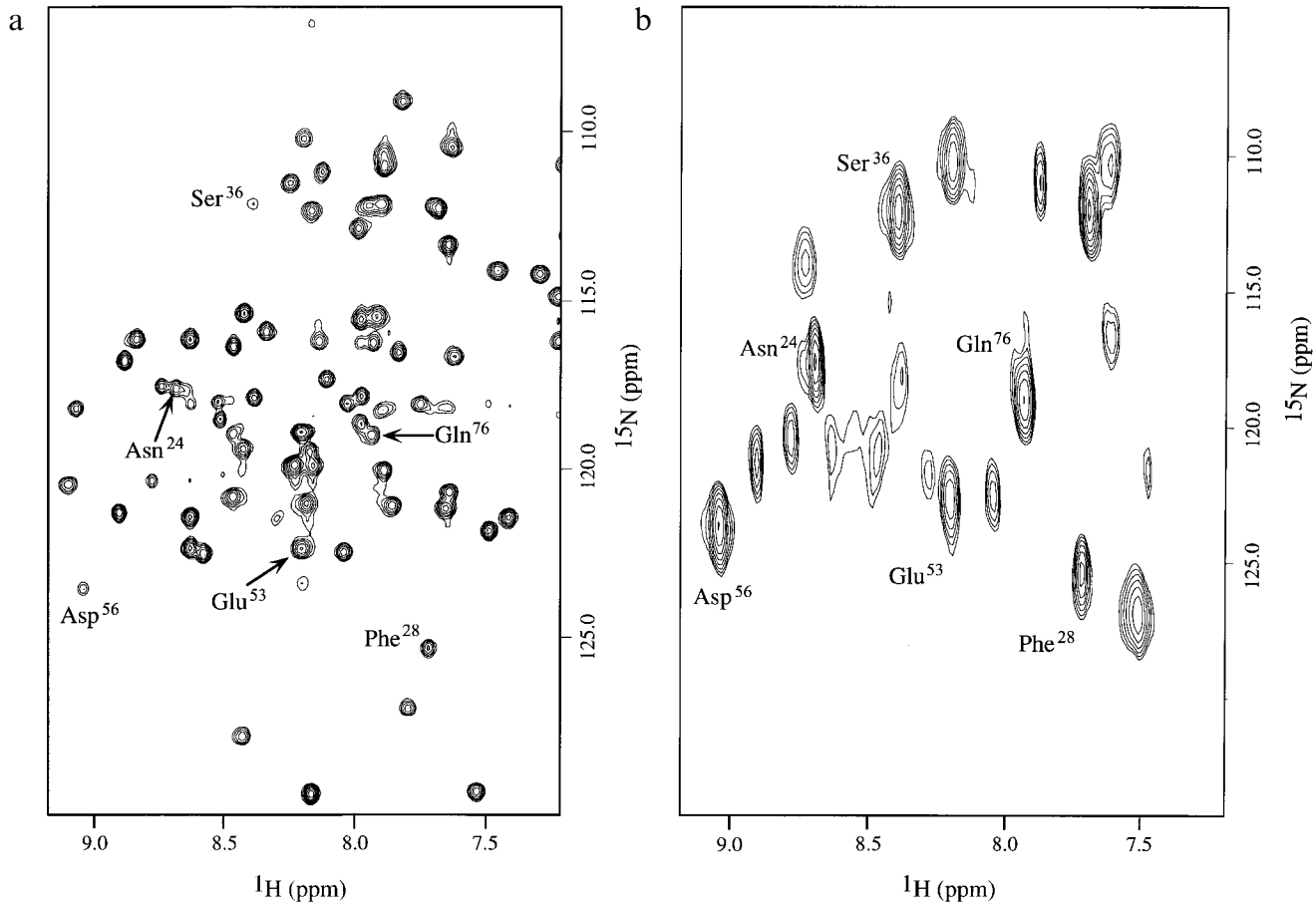

Fig. 5. Comparison of a selected region of the gradient coherence-selected HSQC spectrum of ACP (a) and the $t_m = 60$ ms spectrum collected using the selective-inversion exchange pulse sequence of Kriwacki et al. (1993) (b). The very broad line widths in the indirect dimension of spectrum (b) are an artifact of the window function used on the highly truncated data (see the Materials and Methods section). The intense peak appearing at 7.5 ppm proton and 126 ppm nitrogen shift in spectrum (b), but not visible in spectrum (a), is due to the guanidino group of Arg[4].

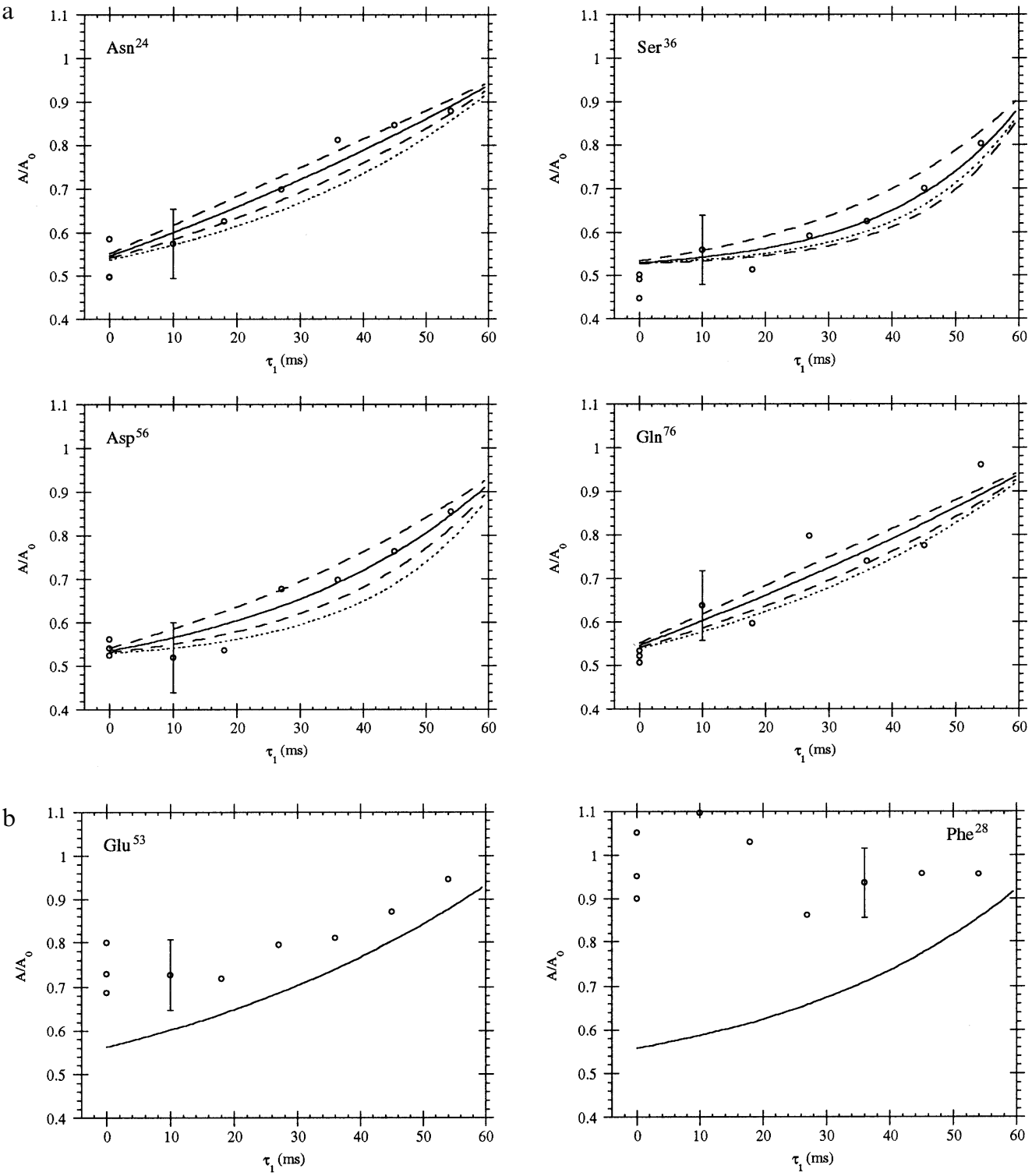

Fig. 6. Representative experimental diffusion attenuation profiles as a function of τ_1. Each data point corresponds to a ratio of signal intensities from a pair of two-dimensional spectra acquired using a nominal gD of 29.0 and 2.9 G/cm, respectively. (a) Experimental diffusion attenuations for four backbone amide protons which are consistent with simple two-site exchange with bulk water. The error in the attenuation factors was estimated to be equal to the standard deviation of the Phe[28] data below, and is indicated by the error bar. The theoretical curves shown as solid and dashed lines correspond to the mean and 1σ error bars of the rate estimated by fitting the data to Eq. A8 assuming a gradient strength of 31 G/cm, and protein and water diffusion coefficients of 0.1 and 2.2 μm^2/ms, respectively (see the text). Error estimates for the rates were determined by Monte Carlo simulation. For comparison, the predicted attenuation profiles based on the exchange rates measured using a selective-inversion exchange experiment are shown as dotted lines. (b) Experimental diffusion attenuations for two backbone amide protons which have significant contributions from intramolecular cross-relaxation. The predicted attenuation profiles based on the exchange rates measured using a selective-inversion exchange experiment are shown.

of sucrose in D_2O (Gosting and Morris, 1949). All spectra were acquired at a temperature of 25 °C.

Selective-inversion exchange measurements using a heteronuclear (^1H-^{15}N) multiple quantum element for detection were obtained using the pulse sequence described in our previous work (Andrec et al., 1995). Since the degree of ^{15}N chemical shift degeneracy is minimal in these spectra, only 19 complex points were acquired in the indirect dimension. Diffusion experiments were performed using the pulse sequence of Fig. 1, with only 16 complex points in the indirect dimension. Note that care must be taken to avoid artifacts due to the loss of magnetization because of radiation damping of the intense water signal. This is done by including spoil gradients at the start of any delay in which the signal of interest is stored along the negative z-axis. These gradients (g1 and g2) have been placed asymmetrically along axes orthogonal to that used for the diffusion gradient to prevent the gradient recall of water magnetization during acquisition. In addition, the diffusion experiment depicted in Fig. 1 is never performed with gD exactly zero to prevent radiation damping of water during the spin echo. Thus, data were only collected using 10% and 100% of the maximum gradient strength to prevent distortion of the profile of the attenuation as a function of τ_1.

Spectral data were processed using the program FELIX (v. 2.3 and 95.0, Biosym Technologies, San Diego, CA, U.S.A.). Zero-filling, skewed sine-bell apodization, and Fourier transformation of the data were followed by quantitation using both nonlinear curve fitting of vectors parallel to the proton dimension at the intensity maximum in the nitrogen dimension, and integration of the two-dimensional cross peaks. Exchange rates were determined from the selective-inversion buildup data by a nonlinear least-squares fit to the functional form

$$A(1 - e^{-kt_m})$$

and error estimates were determined from the standard deviation of the frequency-domain noise and Monte Carlo simulation.

Results

Representative two-dimensional heteronuclear correlation spectra of ACP are shown in Fig. 5, where a typical HSQC spectrum is compared to a representative selective-inversion difference spectrum. It is obvious that a large number of the resonances which appear in the HSQC spectrum do not appear in the selective-inversion difference spectrum. This is not surprising, since an amide proton must be exchanging rapidly with the solvent or be within a distance suitable for cross-relaxation with a spin whose chemical shift is degenerate with that of water (such as an α-proton) in order to provide detectable magnetization at the amide site. It is also apparent that some of the stronger peaks in Fig. 5b, such as Asp^{56} and Ser^{36}, are weak in Fig. 5a due to exchange. The possibilities of exchange versus cross-relaxation may be distinguished by a comparison of intensities in a selective-inversion ROE spectrum (Kriwacki et al., 1993) or by means of a relaxation filter such as that recently proposed by Mori et al. (1996). Alternatively, we may use the diffusion/exchange experiment proposed here to accomplish the same goal.

For the new approach, two difference spectra were acquired for each of seven different values of τ_1 using the sequence of Fig. 1, one using a gD gradient of 10% of the maximum power and the other at maximum gradient power. The total acquisition time for each difference spectrum was approximately 6 h. These pairs of spectra were used to calculate diffusion attenuation factors at each value of τ_1. Data for four amino acid residues in ACP which have good signal-to-noise ratios in the selective-inversion spectra (greater than 600:1) and no significant spectral overlap are shown in Fig. 6a. It was confirmed that the exchange signal for these four residues arises from exchange rather than cross-relaxation with a spin whose resonance is under water using both rotating-frame and relaxation-filter experiments (data not shown).

The numerical evaluation of the exchange rates from the diffusion data would require accurate knowledge of the diffusion coefficients, especially D_w, and the field-gradient strength g. However, the accurate calibration of the maximum gradient strength is difficult, and it is not clear that the diffusion coefficient of 2.2 μm^2/ms for bulk water in the literature (Longsworth, 1960) is appropriate for bulk water in a protein solution. We therefore chose to estimate the product g^2D_w from the experimental data collected in the limit $\tau_1 = 0$. If we then assume a water diffusion coefficient of 2.2 μm^2/ms, we calculate an apparent gradient strength from the $\tau_1 = 0$ data of 31 ± 2 G/cm. Least-squares fits of the exchange rate for each curve were determined using this value of g in Eq. A8 as well as g = 29 and 33 G/cm, in order to assess the effect of errors in g^2D_w on the estimated exchange rates.

An error estimate of 0.08 for the individual attenuation factors was determined from the standard deviation of the attenuations of Phe^{28}. This is a case where we know that magnetization transfer occurs from an α-proton degener-

TABLE 1
COMPARISON OF EXPERIMENTAL AMIDE EXCHANGE RATES DETERMINED USING SELECTIVE-INVERSION AND DIFFUSION-BASED METHODS

Residue	Selective-inversion rate (s^{-1})	Diffusion-based rates (s^{-1})		
		g = 29 G/cm	g = 31 G/cm	g = 33 G/cm
Asn^{24}	22 ± 2	15 ± 10	7 ± 8	3 ± 5
Ser^{36}	60 ± 5	67 ± 15	50 ± 17	17 ± 10
Asp^{56}	50 ± 3	39 ± 15	27 ± 12	17 ± 10
Gln^{76}	19 ± 2	15 ± 11	7 ± 8	2 ± 4

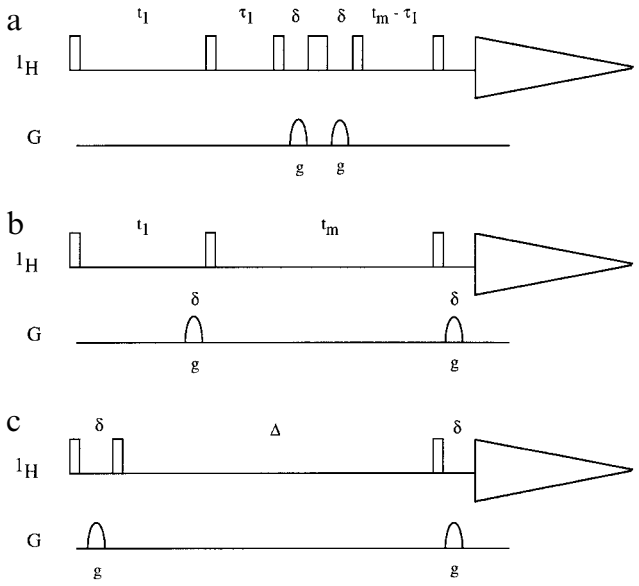

Fig. 7. Schematic illustrations of the three pulse sequences whose characteristics are compared in the Discussion section. (a) The diffusion/exchange method proposed in the present paper, implemented as a homonuclear 2D EXSY. (b) The GEXSY experiment of Moonen et al. (1992). (c) The nonselective stimulated echo diffusion experiment (Tanner, 1970) analyzed by Johnson (1993).

ate with water, and that the diffusion attenuation should be independent of τ_1. Using the standard deviation of the Phe[28] attenuations is likely to be an overestimate of the true error.

The rates resulting from the least-squares fitting of the experimental data and the errors estimated from Monte Carlo error analysis are given in Table 1. The theoretical curves corresponding to the rates from the g = 31 G/cm fits are shown as solid lines in Fig. 6a, bounded by dashed lines corresponding to ±σ. The curves predicted based on rates measured using the selective-inversion exchange experiment are shown as dotted lines in Fig. 6a. The diffusion-filtered experimental data fit the theoretical curves well in all four cases, and while there is a tendency for a small underestimate of the rate in comparison to the selective-inversion data in several cases, the agreement is nearly within the ±σ limits. Choosing a gradient value of 29 G/cm actually achieves total agreement with the selective-inversion data, but causes substantial deviations from experiment at $\tau_1 = 0$. The fits are very insensitive to variations in the diffusion coefficient of the protein. For example, a change in the protein diffusion coefficient by a factor of 3 (from 0.05 to 0.15 μm^2/ms) will only result in a shift of the $\tau_1 = t_m$ intercept by 3% (from 0.985 to 0.957).

In addition to the cases where the experimental data fit a simple two-state model, there are cases where we observe deviations from the theoretically predicted profiles. Some examples, namely Glu[53] and Phe[28], are shown in Fig. 6b. Phe[28] clearly shows the characteristics of domination by an intramolecular cross-relaxation process. The profile of Glu[53] is consistent with a mixture of chemical exchange and cross-relaxation processes.

Discussion

On the whole, the diffusion attenuation profiles for most observable residues agree well with the theoretical predictions based on the independently measured exchange rates (Fig. 6a). However, even in Fig. 6a a small systematic error is observed, and this point is worthy of some discussion. The fits obtained using g = 31 G/cm show a slight underestimate of the exchange rate compared with those determined using selective inversion. One possibility is that this is due to a 'background' transfer of magnetization from protons at the chemical shift of water to the amide protons due to spin diffusion. In this case, one would expect the selective-inversion experiment to overestimate the exchange rate, since the magnetization will build up faster, while one would expect the diffusion-based experiment to underestimate the rate, as more of the observed magnetization will arise from intramolecular pathways which have the diffusion properties of protein. Another possibility is that the discrepancy arises from a misestimate of the gradient strength or diffusion coefficient of water. It is clear from Table 1 that the exchange rate determination is very sensitive to misestimates of the gradient strengths, and that the use of a gradient strength value of 29 G/cm achieves total agreement with the selective-inversion data. However, this produces a large deviation from the theoretical curves at $\tau_1 = 0$, for which we have no physical explanation. The first possibility therefore seems more likely, and the two approaches might be expected to give values which bracket the true value of the exchange rate.

The attenuation profiles of the 'anomalous' residues Glu[53] and Phe[28] (Fig. 6b) are also in agreement with independent experimental data, suggesting that a three-state rather than a two-state model should be used. For Glu[53], both rotating-frame and relaxation-filter experiments confirm that both exchange and cross-relaxation pathways contribute to the signal. The attenuation profile of Phe[28] is independent of τ_1 to within experimental error. This is in agreement with previous isotope-exchange experiments which showed that the amide exchange rate of Phe[28] is too slow to contribute to the signal in a selective-inversion exchange experiment, and that the observed signal is likely to be due to cross-relaxation (Andrec et al., 1995). For both Phe[28] and Glu[53] the α-proton of a spatially proximate residue is nearly degenerate with the water resonance and is likely to be the source of the cross-relaxation. In the residues thus far examined in ACP, we have not identified a case of mediated exchange. This is consistent with the observation of rather small numbers of long-lifetime immobilized water molecules in other proteins, and that such water molecules often play

a structural role (Gerothanassis, 1994; Billeter, 1995; Bryant, 1996). Thus, the lack of evidence for long-lived water molecules in ACP is not surprising, given its rather labile structure (Kim and Prestegard, 1989; Andrec et al., 1995). Nevertheless, we have been able to demonstrate the sensitivity of our experiment to the participation of a third site through cross-relaxation.

Several experimental approaches to the measurement of exchange rates using pulsed-field gradients have appeared thus far in the NMR literature, and it is appropriate to compare the characteristics of our experiment to those methods. Our proposed experiment as well as the previous proposals are shown in schematic form in Fig. 7. It should be noted that although the pulse sequence used in the experimental work described here is based on detection through a heteronuclear correlation element, this is not necessary. In principle, the moveable diffusion filter element described here could be used within the mixing time of a standard homonuclear NOESY/EXSY-type experiment. One of the first methods proposed was the 'GEXSY' experiment of Moonen et al. (1992), a variant of the 2D EXSY experiment in which the diffusion encode and decode gradients flank the mixing period (Fig. 7b). More recently, a variant of this pulse sequence was used by Dötsch and Wider (1995) in an attempt to determine the lifetimes of internal hydration water mol-

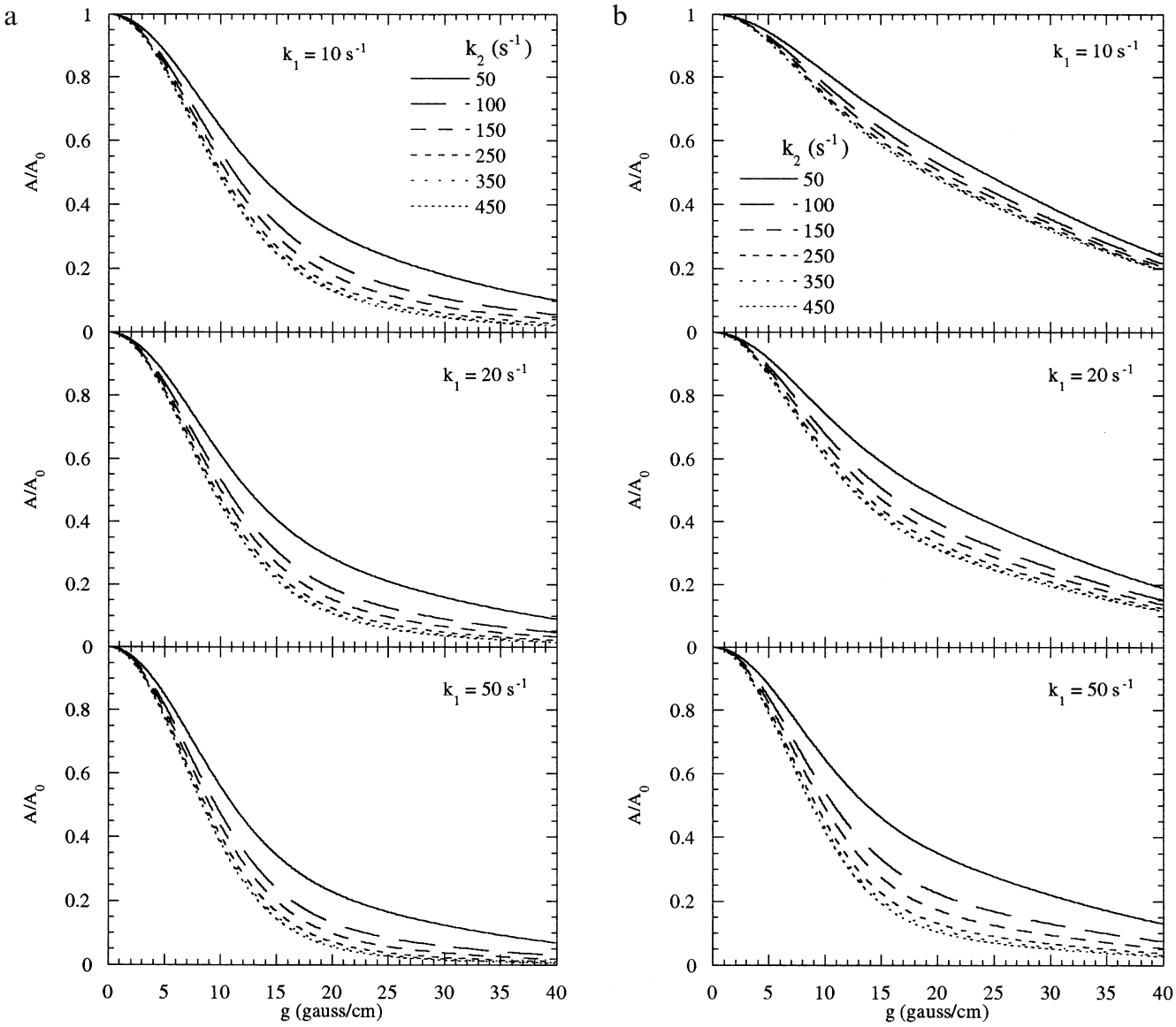

Fig. 8. Theoretically predicted diffusion attenuation profiles as a function of gradient strength and exchange rates k_1 and k_2 for the three-state exchange process shown in Scheme 3 using the GEXSY and nonselective stimulated echo sequences of Figs. 7b and c. The following parameters were used: $t_m = \Delta = 60$ ms, $D_{ab} = 0.1$ μm^2/ms, $D_c = 2.2$ μm^2/ms, $\delta = 4$ ms, and $[C]/[B] = [C]/[A] = 10^4$. (a) Theoretical diffusion attenuation for the GEXSY experiment calculated using Eq. 2 and the three-state generalization of Eq. 7 with the initial boundary conditions corresponding to the cross peak connecting species B/C and A. (b) Theoretical diffusion attenuation for the nonselective stimulated echo experiment calculated in a similar fashion using the initial boundary conditions corresponding to excitation of all three species and observation of species A.

ecules in proteins. Note, first of all, that in this experiment t_m serves as both a mixing period for the transfer of magnetization between spins, and as the diffusion period in which spins are labeled based on their mobilities. In addition, the diffusion periods in these experiments do not begin with equilibrium magnetization, since they are preceded by a chemical shift evolution period t_1. The second experimental approach is the simple nonselective stimulated echo diffusion experiment (Fig. 7c) analyzed by Johnson (1993). This experiment is fundamentally different from that of Moonen et al. The GEXSY experiment involves the selective transfer of magnetization between two resolved resonances that begin with chemical shift- and relaxation-modulated amplitudes, while the Johnson analysis assumes that the diffusion period begins with equilibrium magnetization, and that the two resonances are unresolved. Secondly, it is important to note that Moonen et al. implicitly assume that one of the two species (water, in their case) is in vast excess.

To compare the effectiveness of our experiment to that of the GEXSY and nonselective stimulated echo experiments, the diffusion attenuations as a function of gradient strength for the exchange process of Scheme 3 were calculated. Moonen et al. arrive at the following expression for the diffusion attenuation of an amide/water cross peak in a GEXSY experiment:

$$\frac{A}{A_0} = \frac{k\left(\Psi_B - \Psi_A e^{-kt_m}\right)}{\left(1-e^{-kt_m}\right)\left[k-\gamma^2 g^2 \delta^2 \left(D_B - D_A\right)\right]} \qquad (6)$$

where $\Psi_i = \exp(-\gamma^2 g^2 \delta^2 D_i t_m)$, and we have used the notation presented in the Theory section. However, this result is difficult to generalize to a three-state system. The formalism proposed by Johnson (1993) is much more convenient in this regard. It recognizes that the effect of diffusion can be included as a relaxation term in the standard exchange matrix approach. Thus, for two exchanging species one can use Eq. 2 with an exchange matrix given by

$$\mathbf{K} = \begin{pmatrix} k_f + \gamma^2 g^2 \delta^2 D_A & -k_r \\ -k_f & k_r + \gamma^2 g^2 \delta^2 D_B \end{pmatrix} \qquad (7)$$

If the two components cannot be resolved in chemical shift, then the results obtained using this approach for the nonselective diffusion experiment are consistent with the previous results of Kärger et al. (1988). However, this approach is quite general and can be used to calculate the diffusion attenuations for a variety of pulse sequences for which the narrow-gradient approximation is valid by the use of the proper boundary conditions.

The results of the calculations for the GEXSY and nonselective stimulated echo experiments are shown in Fig. 8. A comparison of the dispersion in attenuation factors as a function of k_1 and k_2 with that in Fig. 4 shows that the rates can be resolved to a comparable degree. However, this dispersion is only evident at quite large attenuations ($A/A_0 \approx 0.3$). This could be a serious disadvantage when sensitivity is at a premium, either due to slow exchange rates or to low sample concentrations. Of course, the overall attenuation could be decreased by using a shorter mixing time or δ, but only at a loss of sensitivity or exchange rate resolution. It should be emphasized that the curves of Figs. 4 and 8 were calculated using the same total mixing time; therefore, the overall sensitivity of both experiments should be directly comparable.

The experiment of Fig. 1 differs most from the previous experiments in the literature in that the mobilities of the exchanging spins are sampled only during a window of length 2δ which is small compared to the total mixing period. By sliding this window through the mixing period, the course of the exchange process can be monitored in terms of the translational mobilities of the species involved, effectively uncoupling the exchange measurement from the diffusion measurement. By contrast, the diffusion attenuation obtained using either the GEXSY or the nonselective stimulated echo experiment as a function of gradient strength is determined by the total mean-square displacement experienced by an observed spin during the entire time period t_m or Δ, resulting in a superposition of decaying exponentials which couple the exchange and diffusion in a less trivial manner.

To summarize, we have shown that the experiment of Fig. 1 can be used to determine exchange rates by means of diffusion measurements. For the case of simple two-state exchange, the results obtained using this experiment approximate those obtained using the more traditional method of selective-inversion exchange. We have also demonstrated that this experiment could, in principle, be used to determine exchange rates in more complex processes, where the rates could not be determined using only traditional methods based on magnetization transfer. The characteristics of this experiment are shown to differ significantly from the experiments previously proposed in the literature. These differences may offer advantages in terms of sensitivity and ease of analysis.

Acknowledgements

M.A. would like to thank Eric W. Sayers for many helpful discussions. This work was supported by the National Institutes of Health, Grant GM33225.

References

Allerhand, A. and Gutowsky, H.S. (1965) *J. Chem. Phys.*, **42**, 4203–4212.

Altieri, A.S., Hinton, D.P. and Byrd, R.A. (1995) *J. Am. Chem. Soc.*, **117**, 7566–7567.

Andrec, M., Hill, R.B. and Prestegard, J.H. (1995) *Protein Sci.*, **4**, 983–993.

Billeter, M. (1995) *Prog. NMR Spectrosc.*, **27**, 635–645.

Bloom, M., Reeves, L.W. and Wells, E.J. (1965) *J. Chem. Phys.*, **42**, 1615–1624.
Bryant, R.G. (1996) *Annu. Rev. Biophys. Biomol. Struct.*, **25**, 29–53.
Chen, A.D., Wu, D.H. and Johnson Jr., C.S. (1995) *J. Phys. Chem.*, **99**, 828–834.
Dingley, A.J., Mackay, J.P., Chapman, B.E., Morris, M.B., Kuchel, P.W., Hambly, B.D. and King, G.F. (1995) *J. Biomol. NMR*, **6**, 321–328.
Dötsch, V. and Wider, G. (1995) *J. Am. Chem. Soc.*, **117**, 6064–6070.
Englander, S.W. and Kallenbach, N. (1984) *Q. Rev. Biophys.*, **16**, 521–655.
Gemmecker, G., Jahnke, W. and Kessler, H. (1993) *J. Am. Chem. Soc.*, **115**, 11620–11621.
Gerothanassis, I.P. (1994) *Prog. NMR Spectrosc.*, **26**, 171–237.
Gillespie, D.T. (1992) *Markov Processes: An Introduction for Physical Scientists*, Academic Press, San Diego, CA, U.S.A.
Gosting, L.J. and Morris, M.S. (1949) *J. Am. Chem. Soc.*, **71**, 1998–2006.
Grzesiek, S. and Bax, A. (1993) *J. Biomol. NMR*, **3**, 627–638.
Hahn, E.L. (1950) *Phys. Rev.*, **80**, 580–594.
Hill, R.B., MacKenzie, K.R., Flanagan, J.M., Cronan, J.E. and Prestegard, J.H. (1995) *Protein Expr. Purif.*, **6**, 394–400.
Hinton, D.P. and Johnson Jr., C.S. (1993) *J. Phys. Chem.*, **97**, 9064–9072.
Johnson Jr., C.S. (1993) *J. Magn. Reson.*, **A102**, 214–218.
Kärger, J., Pfeifer, H. and Heink, W. (1988) *Adv. Magn. Reson.*, **12**, 1–89.
Kim, Y. and Prestegard, J.H. (1989) *Biochemistry*, **28**, 8792–8797.
Kriwacki, R.W., Hill, R.B., Flanagan, J.M., Caradonna, J.P. and Prestegard, J.H. (1993) *J. Am. Chem. Soc.*, **115**, 8907–8911.
Lin, M. and Larive, C.K. (1995) *Anal. Biochem.*, **229**, 214–220.
Longsworth, L.G. (1960) *J. Phys. Chem.*, **64**, 1914–1917.
Moonen, C.T.W., Van Gelderen, P., Vuister, G.W. and Van Zijl, P.C.M. (1992) *J. Magn. Reson.*, **97**, 419–425.
Mori, S., Berg, J.M. and Van Zijl, P.C.M. (1996) *J. Biomol. NMR*, **7**, 77–82.
Morris, K.F. and Johnson Jr., C.S. (1992) *J. Am. Chem. Soc.*, **114**, 3139–3141.
Morris, K.F. and Johnson Jr., C.S. (1993) *J. Am. Chem. Soc.*, **115**, 4291–4299.
Moseley, H.N.B., Curto, E.V. and Krishna, N.R. (1995) *J. Magn. Reson.*, **B108**, 243–261.
Pauly, J., Le Roux, P., Nishimura, D. and Macovski, A. (1991) *IEEE Trans. Med. Imaging*, **10**, 53–65.
Press, W.H., Teukolsky, S.A., Vetterling, W.T. and Flannery, B.P. (1992) *Numerical Recipes in C: The Art of Scientific Computing*, Cambridge University Press, Cambridge, U.K.
Sandström, J. (1982) *Dynamic NMR Spectroscopy*, Academic Press, London, U.K.
Shaka, A.J., Barker, P.B. and Freeman, R. (1985) *J. Magn. Reson.*, **64**, 547–552.
Shinnar, M., Elff, S., Subramanian, H. and Leigh, J.S. (1989) *Magn. Reson. Med.*, **12**, 75–80.
Stejskal, E.O. and Tanner, J.E. (1965) *J. Chem. Phys.*, **42**, 288–292.
Stepisnik, J. (1981) *Physica B*, **104**, 350–364.
Tanner, J.E. (1970) *J. Chem. Phys.*, **52**, 2523–2526.
Tolman, J.R., Chung, J. and Prestegard, J.H. (1992) *J. Magn. Reson.*, **98**, 462–467.
Van Kampen, N.G. (1961) *Can. J. Phys.*, **39**, 551–567.

Appendix

The calculation of the effect of exchange during the spin echo on the diffusion attenuation is, in general, nontrivial. However, if there is a large difference in concentrations between the exchanging species, then a closed-form solution can be obtained. We derive this result for the two-state and three-state exchange processes shown in Schemes 1 and 3. If the concentrations of the exchanging species are comparable, then the effective diffusion attenuations may be calculated using a Monte Carlo approach.

We first consider the two-state exchange process of Scheme 1. The expected diffusion attenuation as a function of τ_1 can be determined by considering a time average over all possible exchange events which can lead to an observable signal, weighted by their probability. For a $B \rightarrow A$ exchange event to contribute to an observable signal in the selective-inversion difference experiment, this exchange event must occur in the forward direction in the time period between the selective pulse and the start of the HMQC, and it must not be reversed by an $A \rightarrow B$ exchange event. Because of the vast excess of species B, we can assume that if a spin leaves A it will never return, and that a spin entering A from B has spent its entire previous existence on B. Suppose that such an exchange event occurs at a time t' after the selective-inversion pulse. If we assume that exchange events are distributed according to a Poisson process, then the probability density that a $B \rightarrow A$ exchange event occurs in a time interval dt is k, and the probability density that no exchange events occur in the time interval $(t_m + 2\delta - t')$ is proportional to $\exp[-k(t_m + 2\delta - t')]$, where k is the rate of $A \rightarrow B$ exchange. When normalized over the duration of the mixing period $0 \le t \le t_m + 2\delta$, the probability density that an exchange event at time t' will lead to an observable signal is

$$S(t') = \frac{k e^{-k(t_m+2\delta-t')}}{1-e^{-k(t_m+2\delta)}} \qquad (A1)$$

The insertion of a spin echo diffusion element at time τ_1 will cause the signal arising from exchange events before and after τ_1 to contribute differently to the observed signal. Therefore, we consider the signal arising from exchange events during the τ_1 and τ_2 intervals separately. The fractions of the signal arising from exchange before, during, and after the spin echo are

$$F_1(\tau_1) = \int_0^{\tau_1} S(t)\,dt = \frac{e^{-k(t_m+2\delta)}\left(e^{k\tau_1}-1\right)}{1-e^{-k(t_m+2\delta)}} \qquad (A2a)$$

$$F_2(\tau_1) = \int_{\tau_1}^{\tau_1+2\delta} S(t)\,dt = \frac{e^{-k(t_m-\tau_1)}\left(1-e^{-2k\delta}\right)}{1-e^{-k(t_m+2\delta)}} \qquad (A2b)$$

and

$$F_3(\tau_1) = \int_{\tau_1+2\delta}^{t_m+2\delta} S(t)\,dt = \frac{1-e^{-k(t_m-\tau_1)}}{1-e^{-k(t_m+2\delta)}} \qquad (A2c)$$

respectively.

For the signal arising from exchange events before the spin echo, the diffusion attenuation will depend only on the mobility of the observed species Ψ_A, while for exchange events after the spin echo, the diffusion attenuation will depend only on the mobility of the inverted species Ψ_B. For exchange events during the spin echo, the diffusion attenuation will be an averaged attenuation $\Psi(t)$ which will depend on the precise time of the exchange event. Therefore, the observed diffusion attenuation is predicted to be the weighted average of the attenuation as a function of exchange time:

$$\begin{aligned}\frac{A(\tau_1)}{A_0(\tau_1)} &= \int_0^{t_m+2\delta} \Psi(t)S(t)\,dt \\ &= \Psi_A F_1(\tau_1) + \Psi_B F_3(\tau_1) \\ &+ \frac{ke^{-k(t_m+2\delta)}}{1-e^{-k(t_m+2\delta)}} \int_{\tau_1}^{\tau_1+2\delta} \Psi(t)e^{kt}\,dt\end{aligned} \qquad (A3)$$

If the narrow-gradient condition is satisfied, then only the first two terms are needed, and Eq. A3 is equivalent to the $p_A \to 0$ limit of Eq. 4. If the narrow-gradient condition is not satisfied, then we must evaluate the last integral in Eq. A3 and consider in detail the time dependence of $\Psi(t)$.

For unrestricted diffusion in the absence of flow, the diffusion attenuation in a spin echo pulse sequence with an arbitrary gradient shape is given by

$$-\ln(\Psi) = \frac{1}{2}\gamma^2 \int_0^{2\delta} dt_1 \int_0^{2\delta} dt_2\; g^*(t_1)g^*(t_2)\langle X(t_1)X(t_2)\rangle \qquad (A4)$$

where g*(t) is the effective gradient as a function of time (which takes into account the effect of any 180° pulses), and the average is over all displacements X(t) (Stepisnik, 1981). To simplify notation, we will assume that $\tau_1 = 0$. Since the timescale of chemical exchange processes is, in all cases of interest, much longer than the correlation time of the diffusion process (10^{-9}–10^{-10} s^{-1}), we can decouple the effects of diffusion and exchange and determine an effective Ψ by averaging Eq. A4 over all possible exchange events. Since we only need to consider one exchange event based on the assumed concentration ratio of species A and B, this average can be determined in closed form. We assume that our gradient pulses fill nearly the entire spin echo delay (as they usually do), making the absolute value of g*(t) a constant. Since we are only interested in processes occurring on a much longer timescale than the diffusion correlation time, we can approximate the diffusion process as a continuous Markov process (Gillespie, 1992) which satisfies the driftless Fokker–Planck equation

$$\frac{\partial}{\partial t} P(X,t|0,0) = 2D(t)\frac{\partial^2}{\partial X^2} P(X,t|0,0) \qquad (A5)$$

where the diffusion propagator P(X,t|0,0) gives the probability of a molecule initially at position 0 at time 0 to be at position X at time t. The solution of Eq. A5 for any arbitrary integrable function D(t) can be easily determined by a transformation of variables (Van Kampen, 1961), and the solution is given by

$$P(X,t|0,0) = \frac{1}{\sqrt{2\pi\theta}} \exp\left(\frac{-X^2}{2\theta}\right)$$

where

$$\theta = \int_0^t D(\tau)\,d\tau$$

In this case,

$$D(t) = \begin{cases} D_B, & 0 \le t < t' \\ D_A, & t' \le t \le 2\delta \end{cases}$$

and we find that the diffusion propagator is given by

$$P(X,t|0,0) = \begin{cases} \dfrac{1}{\sqrt{4\pi D_B t}} \exp\left(\dfrac{-X^2}{4D_B t}\right), & 0 \le t < t' \\ \dfrac{1}{\sqrt{4\pi[D_A(t-t')+D_B t']}} & \\ \times \exp\left(\dfrac{-X^2}{4[D_A(t-t')+D_B t']}\right), & t' \le t \le 2\delta \end{cases}$$

The position autocorrelation in this case is simply the variance of the position at time t_1 (Gillespie, 1992)

$$\begin{aligned}\langle X(t_1)X(t_2)\rangle &= \langle X(t_1)^2\rangle \\ &= \begin{cases} 2D_B t_1, & 0 \le t_1 < t' \\ 2[D_A(t_1-t') + D_B t'], & t' \le t_1 \le 2\delta \end{cases}\end{aligned} \qquad (A6)$$

provided that $t_1 \le t_2$.

For a constant gradient of level g during the spin echo, the effective gradient g*(t) is

$$g^*(t) = \begin{cases} g, & 0 \le t < \delta \\ -g, & \delta \le t \le 2\delta \end{cases}$$

Using the above results, we find

$$\Psi(t')=\begin{cases}\Psi_A \exp\left[\dfrac{-\gamma^2 g^2}{3}(D_B-D_A)t'^3\right], & 0 \le t' < \delta \\ \Psi_B \exp\left[\dfrac{\gamma^2 g^2}{3}(D_B-D_A)(2\delta-t')^3\right], & \delta \le t' \le 2\delta\end{cases} \quad (A7)$$

where the diffusion attenuations in the absence of chemical exchange are

$$\Psi_i = \exp\left(-\frac{2}{3}\gamma^2 g^2 D_i \delta^3\right)$$

We have not taken into account the effect on the spin echo signal of phase offsets due to chemical shift evolution (Bloom et al., 1965) or the presence of scalar couplings (Allerhand and Gutowsky, 1965; Sandström, 1982) in the derivation of Eq. A7. Since we consider only ratios of signals with and without diffusion gradients, the effect of such processes will cancel to first order.

Equation A7 can be substituted for $\Psi(t)$ in the integral of Eq. A3. The result is

$$\int_{\tau_1}^{\tau_1+2\delta} \Psi(t) e^{kt}\, dt =$$

$$\Psi_A \int_{\tau_1}^{\tau_1+\delta} \exp\left[-\frac{1}{3}\gamma^2 g^2 (D_B - D_A)(t-\tau_1)^3 + kt\right] dt$$

$$+ \Psi_B \int_{\tau_1+\delta}^{\tau_1+2\delta} \exp\left[\frac{1}{3}\gamma^2 g^2 (D_B - D_A)(\tau_1 - 2\delta - t)^3 + kt\right] dt$$

and the overall average diffusion attenuation as a function of τ_1 is given by

$$\frac{A(\tau_1)}{A_0(\tau_1)} = Q_1 + Q_2 e^{k\tau_1} \quad (A8)$$

where

$$Q_1 = \frac{\Psi_B - \Psi_A e^{-k(t_m+2\delta)}}{1 - e^{-k(t_m+2\delta)}}$$

and

$$Q_2 = \left(\frac{e^{-kt_m}}{1-e^{-k(t_m+2\delta)}}\right)$$

$$\times\left[\Psi_A e^{-2k\delta}\left(1 + k\int_0^{\delta} \exp\left[-\frac{1}{3}\gamma^2 g^2 (D_B - D_A)t^3 + kt\right] dt\right)\right.$$

$$\left. - \Psi_B\left(1 - k\int_0^{\delta} \exp\left[\frac{1}{3}\gamma^2 g^2 (D_B - D_A)t^3 - kt\right] dt\right)\right]$$

Unfortunately, the integrals in Q_2 cannot be evaluated in terms of any ordinary functions, but numerical evaluation is quite straightforward. A comparison of the attenuations as a function of τ_1 for various exchange rates calculated using Eq. A8 and the $p_A \to 0$ limit of Eq. 4 is shown in Fig. 3.

We may derive the effective diffusion attenuation of species B for the exchange process of Scheme 3 using a similar procedure. Again we will assume that only the last exchange event is relevant to the determination of the diffusion attenuation. Suppose that the final exchange event occurs at a time t from the *end* of the spin echo. The probability of such an event is given by $P(t) = k_2 e^{-k_2 t}$, and the effective diffusion attenuation of species B is given by

$$k_2 \int_0^{\infty} \Psi(2\delta - t) e^{-k_2 t}\, dt = \Psi_{ab} e^{-2\delta k_2}$$

$$+ k_2 \Psi_c \int_0^{\delta} \exp\left[\frac{1}{3}\gamma^2 g^2 (D_c - D_{ab})t^3 - k_2 t\right] dt \quad (A9)$$

$$+ k_2 \Psi_{ab} \int_{\delta}^{2\delta} \exp\left[-\frac{1}{3}\gamma^2 g^2 (D_c - D_{ab})(2\delta - t)^3 - k_2 t\right] dt$$

Note that we have neglected any τ_1 dependence of the diffusion attenuation. This is reasonable if $1/k_2 \ll t_m$ (see below).

If there is no large difference in concentrations between the exchanging species, then the assumption underlying the above derivation is no longer valid. However, we can obtain a numerical solution by means of a Monte Carlo-type calculation. If the mean lifetimes are small compared to t_m, then the exchange events during the spin echo will not be correlated with the state of the spin at time $t = t_m$, and we may consider the effective spin echo diffusion attenuation to be independent of τ_1, except for $\tau_1 \approx t_m$. In this case, we may determine an effective diffusion attenuation by generating stochastic exchange events during the spin echo, calculating the diffusion attenuation using an appropriate generalization of Eq. A7, and determining the average over all simulated exchange events. If the mean lifetimes are comparable in magnitude to t_m, then the spin echo diffusion attenuation is no longer independent of τ_1, since one must consider which exchange events during the spin echo will contribute to the signal. The Monte Carlo approach would then involve simulation of exchange events during the entire mixing period.